

ANOMALOUS X-RAY TRANSMISSION BY A QUARTZ SINGLE CRYSTAL

by

JESUDAS MWANJE

B. Sc., University of East Africa, Makerere, 1966

---

A THESIS

submitted in partial fulfillment of the

requirements for the degree

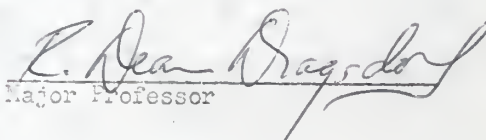
MASTER OF SCIENCE

Department of Physics

KANSAS STATE UNIVERSITY  
Manhattan, Kansas

1968

Approved by:

  
Major Professor

LD  
2668  
T4  
1968  
M893  
C. 2

11

# TABLE OF CONTENTS

	Page
INTRODUCTION . . . . .	1
OUTLINE OF THE DYNAMICAL THEORY OF X-RAY DIFFRACTION . . . . .	h
Nomenclature . . . . .	h
CALCULATION OF EPSILONS FROM THE DYNAMICAL THEORY . . . . .	11
EXPERIMENTAL PROCEDURE . . . . .	15
Preparation of the Crystal . . . . .	15
Crystal Orientation . . . . .	15
ANALYSIS OF EXPERIMENTAL RESULTS . . . . .	20
DISCUSSION . . . . .	30
SUMMARY . . . . .	33
ACKNOWLEDGMENT . . . . .	35
REFERENCES . . . . .	36

## LIST OF TABLES AND PLATE

	Page
Table I. Parameters for calculating the imaginary parts of the atomic scattering factors . . . . .	12
Table II. Calculated imaginary parts of the atomic scattering factors for the five reflections . . . . .	13
Table III. Calculated values of $\epsilon$ for the five reflections . . . . .	14
Plate I. Lang Topograph . . . . .	17
Table IV. Procedure for calculating $Q_\alpha$ and $Q_\beta$ using $(3\bar{3}01)$ planes for illustration . . . . .	23
Table V. Summary of quantities for the $(3\bar{3}01)$ planes, to be plotted on a graph . . . . .	24
Table VI. Summary of experimental and theoretical values of epsilons for each reflection . . . . .	30

## INTRODUCTION

When a beam of radiation is sent through a slab of material, the intensity of the beam is attenuated. The general law describing this absorption is commonly known in Optics as Lambert's Law. This law is stated as follows:  $I = I_0 \exp(-\mu x)$ ; where  $I_0$  is the intensity of the beam entering the slab and  $I$  is the intensity of the beam leaving the slab,  $\mu$  is the linear coefficient of absorption for the material and  $x$  is the thickness of the slab.

The absorption of x-ray radiation is due to several processes. Some energy is lost in heating the material. Energetic photons in the incident beam are lost through the photoelectric effect: the energy of these photons is used in removing electrons from the innermost atomic shells of the absorbing material, giving rise to fluorescent x-rays characteristic of the material. There is also the Compton effect in which the incident photons collide with the loosely bound electrons. The photons lose some of their energy to these electrons and are scattered in directions different from their original direction of incidence. Also, the vibration of bound electrons in a simple harmonic way caused by the incident photons gives rise to scattering of the radiation in directions other than that of incidence. This is the Thomson effect. All these processes result in removing or diverting photons from the direction of the incident beam so that the emergent beam is attenuated. The photoelectric effect and the Compton effect contribute most of the attenuation.

Fairly recently (1941), however, Borrmann<sup>3</sup> observed that under suitable arrangement, a thick, nearly perfect single crystal can transmit radiation with greatly reduced attenuation. The abnormally high transmission has come

to be known as "Anomalous Transmission". Within the last ten years this phenomenon has generated much interest as evidenced by a number of experimental and theoretical papers which have been published on this topic.<sup>2,9,10,12</sup>

Anomalous transmission takes place when a crystal is set for Laue diffraction. As early as the beginning of this century, a theory of diffraction of x-rays, now known as the Kinematical Theory, was formulated by Laue and Bragg and others. Briefly, this theory considers crystal lattice points as centers for spherically scattered wavelets produced by the incident plane waves. The intensity due to these wavelets, at a point far from the crystal (compared with the crystal dimensions), is calculated. It is assumed that the index of refraction of any crystal is unity for x-rays and that each scattered wavelet travels through the crystal without being scattered again by other lattice points. It is also assumed that there is no absorption for radiation in the crystal and that there is no interference between the primary and the scattered waves inside the crystal. This theory gives a good explanation of the observed intensities from powder and mosaic crystals. An alternative theory is the "Dynamical Theory" of diffraction.

The way for the Dynamical Theory was paved by Darwin<sup>5</sup> and Ewald<sup>7</sup> when they considered multiple reflections of radiation in a crystal, although both had different approaches. The theory did not attract many people, probably because the simpler kinematical theory adequately accounted for the observations of x-ray diffraction work. However, work with large, nearly perfect crystals, which have only recently become available, has revealed a number of phenomena which can best be explained by the Dynamical Theory. One of these phenomena is anomalous transmission. Consequently, a number of papers have appeared during the last few years reviewing the theory, with some improvements and

extensions. At the same time, a number of papers have been published reporting experimental work done on anomalous transmission of x-rays by centrosymmetric, one-atom type crystals like silicon, germanium and copper.

On the other hand, little experimental work, if any, has been done on non-centrosymmetric, many-atom type crystals. In this thesis an outline of the Dynamical Theory will be given in an effort to lay the groundwork for the calculation of the parameter  $\xi$  (epsilon), whose physical significance will be discussed at the appropriate point, for five different diffracting sets of atomic planes of an alpha-quartz crystal. The experimental investigation which was carried out to determine the same parameter, in an effort to relate theoretical predictions to experimental results, will be described. The correlation of experimental and theoretical determinations will then be discussed.



## OUTLINE OF THE DYNAMICAL THEORY OF X-RAY DIFFRACTION

The treatment to be given here is based on the paper by Batterman and Cole<sup>1</sup>. Only those aspects of the theory which have a direct bearing on the content of this thesis will be discussed. Consider a plane wave of x-rays incident on a crystal. When the wave enters the crystal, it splits into a diffracted wave and an internal incident wave. If the crystal is perfect and sufficiently thick ( $\mu t \gg 1$ ), the diffracted wave and the internal incident wave interfere within the crystal. A crystal is also an absorbing medium with an index of refraction which is very close to but different from unity. Moreover, a crystal is a periodic structure. Therefore, the index of refraction, and hence the dielectric coefficient, is a periodic function of position. The dynamical theory gives the possible wave fields which can exist in such a medium. In particular, these waves must satisfy Maxwell's equations and Bragg's law. The theory also gives the intensities of these waves. The main assumptions of the theory are that the permeability of a crystal is the same as that of free space, and that the anisotropic, complex dielectric coefficient is periodic in the three dimensions.

### Nomenclature

$\lambda$	incident X-ray wavelength
$\theta$	any glancing angle
$\theta_B$	Bragg angle
$I_0$	intensity of incident beam
$I_D$	intensity of diffracted beam in Bragg direction
$\underline{k}_0$	incident wave vector outside crystal
$\underline{k}_i$	incident wave vector inside crystal
$\underline{k}_H$	Bragg diffracted wave vector inside crystal

- $\mu_0$  linear absorption coefficient in forward direction  
 $t$  crystal thickness in incident direction  
 $\underline{H}$  reciprocal lattice vector  
 $F_H$  structure factor  
 $f_n$  total atomic scattering factor for nth atom in unit cell  
 $\kappa$  dielectric coefficient  
 $P$  ( $= 1$  or  $\cos 2\theta$ ) polarization factor  
 $\hat{n}$  unit inward surface normal  
 $\gamma_0$  direction cosine of incident beam with respect to  $\hat{n}$   
 $\gamma_H$  direction cosine of diffracted beam with respect to  $\hat{n}$   
 $t = t_0/\gamma_H$ ,  $t_0$  = thickness of crystal slab  
 $b = \gamma_0/\gamma_H$   
 $\Delta\theta = \theta_B - \theta$   
 $V$  volume of crystal  
 $r_e$  classical electron radius  
 $f = r_e \lambda^2 / \pi V$   
 $R_H$  real part of  $F_H F_H^*$   
 $I_H$  imaginary part of  $F_H F_H^*$

The electron charge density  $\rho$  in a crystal is given by  $\rho(\underline{r}) = (1/V) \sum_H F_H \exp(-2\pi i \underline{H} \cdot \underline{r})$  and the dielectric coefficient,  $\kappa(\underline{r}) = 1 - f \sum_H F_H \exp(-2\pi i \underline{H} \cdot \underline{r}) \dots (1)$

The Laue Equation may be stated as follows:

$$\underline{K}_H = \underline{K}_0 + \underline{H} \dots (2)$$

The electric field vectors  $\underline{E}$ ,  $\underline{D}$  and the magnetic field vectors  $\underline{H}$ ,  $\underline{B}$  are related by the following Maxwell's equations:

$$\nabla \times \underline{E} = - \frac{\partial \underline{B}}{\partial t} = - \mu_0 \frac{\partial \underline{H}}{\partial t}, \quad \mu_0 \text{ is permeability in free space.}$$

$$\nabla \times \underline{H} = \frac{\partial \underline{D}}{\partial t} = \epsilon_0 \frac{\partial (\kappa \underline{E})}{\partial t}, \quad \epsilon_0 \text{ is electric permittivity in free space.} \quad (3)$$



Field vectors satisfying equations (2) and (3) are given by

$$\underline{A} = \exp 2\pi i(\nu t - \underline{K}_0 \cdot \underline{r}) \sum_{\underline{H}} \underline{A}_{\underline{H}} \exp(-2\pi i \underline{H} \cdot \underline{r}) \quad (4)$$

Here the summation is over all Miller indices,  $\underline{A}$  stands for any of the field vectors in equations (3) and  $\underline{A}_{\underline{H}}$  is the corresponding amplitude;  $\underline{r}$  is a position vector inside the crystal.

Substitution of (4) in Maxwell's equations and use of expression (1) for the dielectric coefficient yields, after lengthy manipulations, the following set of equations:

$$\left[ k^2(1 - f_{F_0}) - (\underline{K}_H \cdot \underline{K}_H) \right] \underline{E}_H - k^2 f_{FH} \underline{E}_L + (\underline{K}_H \cdot \underline{E}_H) \underline{K}_H = 0 \quad (5)$$

Here  $k = |\underline{K}_0|$ ,  $F_0$  is the scattered amplitude in the forward direction (or structure factor corresponding to Miller indices 000). Equations (5) give all the wave vectors  $\underline{K}_H$  which can exist in the crystal. When the crystal is set for Laue diffraction, however, all amplitudes  $\underline{E}_H$  are negligible except for the two directions, namely, the incident and Bragg diffracted directions. In this case the following two equations are obtained:

$$\begin{aligned} \left[ k^2(1 - f_{F_0}) - (\underline{K}_0 \cdot \underline{K}_0) \right] \underline{E}_0 - k^2 f_{FH} \underline{E}_H &= 0 \\ -k^2 f_{FH} \underline{E}_0 + \left[ k^2(1 - f_{F_0}) - (\underline{K}_H \cdot \underline{K}_H) \right] \underline{E}_H &= 0 \end{aligned} \quad (6)$$

Parameters  $\xi_0$  and  $\xi_H$  which are related to the variation of the index of refraction in the crystal are now defined by the equations below:

$$\begin{aligned} \xi_0 &= (\underline{K}_0 \cdot \underline{K}_0)^{1/2} - k(1 - (1/2)f_{F_0}) \\ \xi_H &= (\underline{K}_H \cdot \underline{K}_H)^{1/2} - k(1 - (1/2)f_{F_0}) \end{aligned} \quad (7)$$

Here  $(1 - f_{F_0})$  is the average dielectric coefficient in the crystal. Now equations (6) are a pair of homogenous equations in the amplitudes  $\underline{E}_0$  and  $\underline{E}_H$ . For non-trivial solutions the coefficient determinant must vanish. When  $\xi_0$  and  $\xi_H$  are substituted in the resulting secular equation, the result is

the surface equation:

$$\xi_0 \xi_H = (1/4) k^2 P^2 F_H F_H^{-1} r^2 \quad (2)$$

The surface represented by (2) is called the "Dispersion Surface". For a given polarization  $P$ , this equation represents two hyperbolic sheets. These sheets may be considered as the locus of the center of the Ewald sphere in reciprocal space: from any point on the surface permitted wave vectors can be drawn to points  $O$  (incident direction) and  $H$  (diffracted direction) in the reciprocal space.

To account for absorption, the wave vectors  $\underline{K}_O$  and  $\underline{K}_H$  are assumed complex. Therefore,  $\xi_0$  and  $\xi_H$  are also complex. Writing  $\underline{K}_O = \underline{K}_O' - i\underline{K}_O''$ ;  $|\underline{K}_O''| \ll |\underline{K}_O'|$  and  $\underline{F}_O = \underline{F}_O' + i\underline{F}_O''$  equations (7) give

$$\xi_0' = K_O' - k(1 - (1/2)F_O')$$

and  $\xi_0'' = -K_O'' \cos \beta + (1/2)kF_O''$  where  $\beta$  is the angle between  $\underline{K}_O'$  and  $\underline{K}_O''$  as shown in Figure 1.

When  $\xi_0$  is expressed in terms of  $\Delta\theta$ , the deviation from the Bragg angle, it is seen that for large  $\Delta\theta$ ,  $\xi_0 \rightarrow 0$ ; but this is the case when diffraction is negligible also. In this case we have

$$K_O'' \cos \beta = (1/2)kF_O'' - \xi_0'' \rightarrow (1/2)kF_O''$$

Putting  $\underline{K}_O = \underline{K}_O' - i\underline{K}_O''$  in equation (4) and substituting for  $K_O''$  it is seen that the wave solution (4) has an attenuating factor:  $\exp -2\pi((1/2)kF_O'')t$ , where  $t$  is the distance traversed by the wave. Hence the intensity has an attenuating factor  $\exp(-2\pi kF_O''t)$ . The linear absorption coefficient is then

$\mu_0 = 2\pi kF_O''$ . At the Bragg angle,  $\Delta\theta = 0$ , it is found that

$\xi_0'' = (1/2)k|F_O'| \sqrt{1 - (F_H F_H^{-1})^{1/2}} > 0$ . In this case  $K_O'' \cos \beta$  is less than in the non-Bragg case, which implies reduced absorption.

It was stated that the permitted wave vectors could be drawn from any point on the dispersion surface to the point  $O$  in the direction of incidence

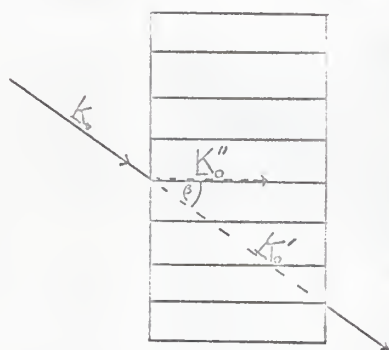


FIG. 1. The real and imaginary parts of the incident wave vector inside the crystal. The real part  $K'_0$  is in the direction of incidence, the imaginary part  $K''_0$  is parallel to the diffracting atomic planes. This diagram shows a rectangular crystal slab set for Laue diffraction, that is, when the diffracting planes are perpendicular to the crystal face of incidence.

and to the point  $H$  in the direction of diffraction (Ewald construction). However, the boundary conditions allow only a limited number of points on the dispersion surface. As the departure from unity of the index of refraction for X-rays is of the order of  $10^{-5}$ , reflection is negligible and it is assumed that the electric and magnetic field vectors cross the crystal plane surface without change in amplitude or frequency. This requirement gives rise to a relationship between the outside incident wave vector and the wave vectors inside the crystal. When these conditions are matched, the wave solution (4) is found to have an attenuating factor  $\exp(-2\pi \underline{K}_0'' \cdot \underline{r})$  and in this case the absorption coefficient is  $\mu_n = 4\pi \underline{K}_0''$  along the normal to the crystal surface, and  $\mu = \mu_n \cos \beta$  along an arbitrary direction of propagation.

When  $\underline{K}_0''$  is expressed in terms of the structure factors and the symmetric Laue setting assumed, one finds

$$\mu = \mu_0 \left( 1 - \frac{|P| I_H}{2 F_0^2 R_H^2 / 2} \right)$$

The parameter  $\epsilon$  is defined as  $\epsilon = \frac{I_H}{2 F_0^2 R_H^2 / 2}$ . Thus,  $\mu = \mu_0 (1 - |P| \epsilon)$ . This shows that the average linear absorption coefficient  $\mu_0$  is reduced by the term  $|P| \epsilon$ , where  $P = 1$  for  $\sigma$ -polarization and  $P = \cos 2\theta$  for  $\pi$ -polarization. Thus,  $\epsilon$  is a measure of the reduction in the absorption when a crystal is set for Laue diffraction. This parameter, by its very definition, depends on the set of the diffracting planes lying between zero and unity. For centrosymmetric, one-atom-type crystals,  $\epsilon$  is very close to unity. This then is the explanation of the anomalous transmission given by the dynamical theory.

Physically, the bigger the amplitude of the electric field vector at an atom, the more the atom absorbs. So, if absorption is reduced so greatly, it follows that the wave field is established in the crystal such that the atom sites occupy the nodal planes. This is what happens in a centrosymmetric

crystal, but for a non-centrosymmetric crystal, like quartz, some atoms can lie off the nodal planes. Consequently, the reduction in absorption is somewhat less than in the centrosymmetric case. The existence of fixed nodal planes inside the crystal implies that standing waves are established between the set of diffracting atomic planes, and the energy propagates along the planes in a way similar to the propagation of energy through wave guides.

On further investigation of the dynamical theory, Dragsdorf and Dreiling<sup>6</sup> were able to obtain a convenient expression for the Bragg diffracted integrated intensity, given below, for unpolarized radiation:

$$S_H = \frac{e^2 \lambda^2}{2mc^2} \frac{\exp -(\mu_0 t + M)}{b^{1/2} v \sin 2\theta} |F_H| [I_0(K) + PI_0(FK)] \quad (9)$$

In this expression  $\exp(-M)$  is the Debye-Waller temperature factor;  $I_0(x)$  is the modified Bessel function of the first kind and zeroth order;  $k = \mu_0 t \epsilon$ .

Further,  $S_H = \frac{E\omega}{S_0}$ , where  $\omega$  is the angular velocity with which the device used to detect the diffracted intensity rotates through the Bragg angle,  $E$  is the power entering the detector and  $S_0$  is the incident intensity on the crystal. When an automatic recorder is connected to the detector, intensity curves are traced out and the areas under these curves are proportional to  $E$ . If  $\omega$  is constant, then the ratio of these areas is the ratio of the integrated intensities. This fact was employed to analyze the experimental data as will be shown in the section on data analysis.



# CALCULATION OF EPSILONS FROM THE DYNAMICAL THEORY

The structure factor of a crystal is given by  $F_H = \sum_n f_n \exp 2\pi i(hx_n + ky_n + lz_n)$  where  $f_n$  is the scattering factor of the  $n^{\text{th}}$  atom in the crystal unit cell and  $x_n, y_n, z_n$  are the fractional coordinates of the atom. Now,  $f_n = f_{on} + \Delta f'_n + i\Delta f''_n$  where  $f_{on}$  is the scattering factor for the stationary atom  $n$ ,  $\Delta f'_n$  is the resonance term (negligible for wavelengths different from the absorption edge of the atom) and  $\Delta f''_n$  is the absorption term. The stationary term  $f_{on}$  is assumed to be the same for all atoms of the same type. When the resonance term is ignored, one has

$$F_H = \sum_n (f_{on} + i\Delta f''_n) \exp 2\pi i(hx_n + ky_n + lz_n)$$

The values (real)  $f_{on}$  were obtained from Cullity<sup>4</sup> for both the silicon and oxygen atoms in quartz. The imaginary parts  $\Delta f''_n$  were calculated as follows:  $\Delta f'' = \sum_j Z_j \eta_j f_{oj}$  where  $Z_j$  is the number of electrons in the  $j^{\text{th}}$  shell and  $\eta_j$  is related to the absorption of energy by the oscillating electric dipole.

From Parratt and Hempstead's paper<sup>13</sup> one finds that

$$\begin{aligned} Z_j \eta_j &= (\pi/2) g_j (\lambda/\lambda_j)^{P_j-1} (P_j - 1) \text{ for } \lambda_j > \lambda \\ &= 0 \text{ for } \lambda_j < \lambda \end{aligned}$$

Here  $\lambda$  is the applied wavelength

$\lambda_j$  is the absorption edge wavelength

$g_j$  is the oscillator strength for all  $j$  electrons

$P_j$  is the weighting factor for the number of electrons in the  $j^{\text{th}}$  shell

In all cases considered here  $\lambda_j > \lambda$ . Table I shows the quantities which were used to compute the imaginary parts of the scattering factors. The electron scattering factors  $f_{oj}$  were obtained from Freeman's<sup>8</sup> curves.



Table I. Parameters for calculating the imaginary parts of the atomic scattering factors

$\lambda = 1.5412 \text{ \AA} \text{ (CuK}\alpha\text{)}$	SILICON				OXYGEN			
	K	L <sub>1</sub>	L <sub>2</sub>	L <sub>3</sub>	K	L <sub>1</sub>	L <sub>2</sub>	L <sub>3</sub>
$\lambda_j \text{ (}\text{\AA}\text{)}$	6.745	62.2	126.5	1942	23.32	326.2	1418	0.00109
$\lambda_j / \lambda_j$	0.2285	0.0214	0.0122	0.000794	0.0660	0.00458		
$P_j \sigma_j$	11/4	2	5/2	5/2	11/4	2	5/2	
	1.33	1.5	4	20	1.33	1.5	4	
$Z_j \eta_j$	0.2757	0.05719	0.0127	0.001055	0.03226	0.0108		0.00034

Using these values of  $Z_j \eta_j$  shown in Table I and the values of  $f_{Oj}$  from the Freeman curves, the imaginary parts for each reflection shown in Table II were found.

Table II. Calculated imaginary parts of the atomic scattering factors for the five reflections

Reflection	$\Delta f''$		$F_o''$
	Silicon	Oxygen	
1100	0.3438	0.0416	1.30
1101	0.3414	0.0407	1.30
1102	0.3360	0.0379	1.30
2203	0.3210	0.0332	1.30
3301	0.3210	0.0332	1.30

Wyckoff<sup>15</sup> gives the fractional coordinates of silicon and oxygen in a unit cell of  $\alpha$ -quartz to be

Si:  $(u00)$ ,  $(\bar{u}\bar{u}1/3)$ ,  $(0u2/3)$

O:  $(xyz)$ ,  $(y-x, x, z + 1/3)$ ,  $(\bar{y}, x - y, z + 2/3)$ ,  $(x - y, \bar{y}, \bar{z})$ ,  
 $(y, x, 2/3 - z)$ ,  $(\bar{x}, y - x, 1/3 - z)$ .

Here  $u = 0.465$ ,  $x = 0.415$ ,  $y = 0.272$ ,  $z = 0.120$ , and the lattice constants are:  $a = 4.90\text{\AA}$ ,  $c = 5.39\text{\AA}$ .

Using these coordinates, the structure factors were computed for each set of planes and from the defining equation,  $\epsilon$  was computed for each set of planes and the results are shown in Table III.

Table III. Calculated values of  $\epsilon$  for the five reflections

Reflection	$I_H$	$R_H^{1/2}(\approx  F_H )$	$\epsilon$
$1\bar{1}00$	10.63	14.81	0.276
$1\bar{1}01$	66.68	37.26	0.686
$1\bar{1}02$	5.98	8.00	0.287
$2\bar{2}03$	28.26	16.60	0.655
$3\bar{3}01$	61.02	30.30	0.774

The same values of  $\epsilon$  were obtained for the  $\text{CuK}_\alpha$  wavelength, showing that this parameter is independent of wavelength for  $\lambda_j > \lambda$ .

## EXPERIMENTAL PROCEDURE

### Preparation of the Crystal

A nearly perfect rectangular crystal of  $\alpha$ -quartz, with  $(11\bar{2}0)$  planes parallel (X-cut) to the large faces of the crystal, was obtained from the Bell Laboratories. To achieve sufficient transmission, the crystal was sliced into two pieces with a diamond saw. One piece was then polished, starting with rather coarse sandpaper to remove the wedge caused by the saw, and moving down to finer sandpaper, then to polishing alumina powder and finally to polishing felt. The crystal was then etched for a few minutes in HF acid; no vigorous reaction was observed. The finished crystal was 0.0626 cm thick, with a maximum of 4 per cent variation from the mean.

A Laue topograph of the finished crystal was taken to examine the degree of perfection of the crystal. Plate I shows the topograph.

### Crystal Orientation

It was planned to obtain reflections from the following sets of atomic planes:  $(1\bar{1}01)$ ,  $(1\bar{1}00)$ ,  $(3\bar{3}01)$ ,  $(2\bar{2}03)$  and  $(1\bar{1}02)$ . All these planes are perpendicular to the planes  $(11\bar{2}0)$  which are parallel to the crystal face. This is necessary for the symmetrical Laue setting which was employed in this investigation. To determine the angles between the surface normal and the normal of each of these planes, a Laue back reflection photograph was taken. The spots due to these planes were identified and the angles were computed using the formula:

$$\cos \phi = \frac{\vec{H}_1 \cdot \vec{H}_2}{|\vec{H}_1| |\vec{H}_2|}, \quad \phi = \text{angle between planes with reciprocal vectors } \vec{H}_1 \text{ and } \vec{H}_2$$

#### EXPLANATION OF PLATE I

PLATE I shows the Lang Topograph of the crystal which was used in the investigation. This topograph for the  $(1\bar{1}01)$  planes shows no obvious internal or surface imperfections. Pendellosung fringes can be seen towards the edges of the topograph. The phenomenon giving rise to these fringes is well explained by the Dynamical Theory. Dreiling<sup>6</sup> shows beautiful photographs of the fringes and discusses this effect. The existence of these fringes is evidence for the existence of a small wedge in the crystal, and it also shows that the crystal used was of high perfection.

## PLATE I





For the hexagonal case,

$$\cos \phi = \frac{h_1 h_2 + k_1 k_2 + (1/2)(h_1 k_2 + h_2 k_1) + l_1 l_2 (3/4) a^2 / c^2}{[h_1^2 + h_1 k_1 + k_1^2 + l_1^2 (3/4) a^2 / c^2]^{1/2} [h_2^2 + h_2 k_2 + k_2^2 + l_2^2 (3/4) a^2 / c^2]^{1/2}}$$

The Bragg angles for these sets of planes for  $\text{CuK}_\alpha$  and  $\text{CuK}_\beta$  radiation were obtained from tables.

To mount the crystal on the diffraction goniometer, an optical goniometer was used initially to obtain a rough adjustment. The crystal was then transferred to the diffractometer. The diffractometer employed in this investigation was the General Electric XRD-6 Unit with a scintillation counter coupled to an automatic recorder through a pulse height selector. The counter support and the specimen support are mechanically coupled such that when the specimen rotates through an angle  $\theta$ , the counter rotates through an angle  $2\theta$ ; this arrangement preserves the focusing conditions. The counter is driven at a constant angular velocity by electric motors with a reversing gear system. The angular position of the counter can be read off the graduated scale provided on the equipment. A copper target tube at a peak voltage of 35 KV and a tube current of 16 mA was used.

Some difficulties were experienced in getting the crystal aligned for diffraction from the desired planes. When these difficulties were overcome, it was found that the diffracted intensities of  $\text{CuK}_\alpha$  and  $\text{CuK}_\beta$  were well resolved, for all the planes under investigation, at an appropriate setting of the pulse height selector.

The diffracted integrated intensities were automatically recorded as the counter scanned through each Bragg angle. The areas under these intensity curves were measured to within a few hundredths of a square inch with a precision planimeter. The curves for the weak intensities from the planes

( $2\bar{2}03$ ) and ( $1\bar{1}02$ ) had rather irregular outlines and were therefore difficult to measure with precision. Using the same peak voltage and tube current and the same pulse height select setting, quartz powder intensities for the same sets of planes under study were obtained and recorded. The areas under these curves were also measured and were used to obtain the ratio of incident  $\text{CuK}_\alpha$  to the  $\text{CuK}_\beta$  components. This will be described further in the section on data analysis.

## ANALYSIS OF EXPERIMENTAL RESULTS

Referring to equation (9) for the integrated intensity,

$$\mathcal{I}_H = \frac{e^2 \lambda^2 |F_H| \exp(-(\mu_0 t + M))}{2mc^2 b^{1/2} V \sin 2\theta} [I_0(k) + P I_0(Pk)]$$

where  $\mathcal{I}_H = \frac{P_0}{\mathcal{I}_0}$ , it is seen that for a constant angular velocity  $\omega$  the ratio of the integrated intensity of the  $\text{CuK}_\alpha$  component to the integrated intensity of the  $\text{CuK}_\beta$  component for a given set of diffracting planes is given by

$$\frac{E_\alpha}{E_\beta} \times \frac{\mathcal{I}_{0\beta}}{\mathcal{I}_{0\alpha}} = \left(\frac{\lambda_\alpha}{\lambda_\beta}\right)^2 \frac{\sin 2\theta_\beta \exp(-\mu_{0\alpha} t_\alpha) [I_0(k_\alpha) + P_\alpha I_0(P_\alpha k_\alpha)]}{\sin 2\theta_\alpha \exp(-\mu_{0\beta} t_\beta) [I_0(k_\beta) + P_\beta I_0(P_\beta k_\beta)]}$$

Now, the power  $E$  entering the counter is proportional to the area under the intensity curve. Let the measured areas corresponding to the peak intensities  $E_\alpha$  and  $E_\beta$  be  $A_\alpha$  and  $A_\beta$ , respectively.

$$\text{Then } \frac{A_\alpha}{A_\beta} \times \frac{\mathcal{I}_{0\beta}}{\mathcal{I}_{0\alpha}} = \left(\frac{\lambda_\alpha}{\lambda_\beta}\right)^2 \frac{\sin 2\theta_\beta \exp(-\mu_{0\alpha} t_\alpha) [I_0(k_\alpha) + P_\alpha I_0(P_\alpha k_\alpha)]}{\sin 2\theta_\alpha \exp(-\mu_{0\beta} t_\beta) [I_0(k_\beta) + P_\beta I_0(P_\beta k_\beta)]}$$

This may be written more compactly as

$$Q_\alpha = K Q_\beta \quad (10)$$

where  $Q_\alpha = I_0(k_\alpha) + P_\alpha I_0(P_\alpha k_\alpha)$ ,  $Q_\beta = I_0(k_\beta) + P_\beta I_0(P_\beta k_\beta)$

$$\text{and } K = \frac{A_\alpha}{A_\beta} \times \frac{\mathcal{I}_{0\beta}}{\mathcal{I}_{0\alpha}} \left(\frac{\lambda_\beta}{\lambda_\alpha}\right)^2 \frac{\sin 2\theta_\alpha \exp(-\mu_{0\beta} t_\beta)}{\sin 2\theta_\beta \exp(-\mu_{0\alpha} t_\alpha)}$$

The only unknown in the expression of  $K$  is the ratio  $\mathcal{I}_{0\beta}/\mathcal{I}_{0\alpha}$ . This was determined from the powder experiment in a manner to be described. The  $Q$ 's are functions of  $\epsilon$  through the relationships  $k_\alpha = \mu_{0\alpha} t_\alpha \epsilon$  and  $k_\beta = \mu_{0\beta} t_\beta \epsilon$ . Therefore, a plot of  $Q_\alpha$  and  $K Q_\beta$  as functions of  $\epsilon$  on the same graph gives a value of  $\epsilon$  which satisfies equation (10). The value of  $\epsilon$  is given by the point where the two curves cross.

The integrated intensity from a powder specimen in the Bragg case is given by

$$P/I_0 = \frac{e^4 \lambda^3 V^2 m^2}{8 \pi m^2 c^4 R} \left( \frac{1 + \cos^2 2\theta}{4 \sin^2 \theta \cos \theta} \right) \frac{\exp(-2\mu t)}{2\mu} |F|^2 \text{ where } P \text{ is the power}$$

entering the detector,  $I_0$  is the incident intensity,  $N$  is the number of atoms per unit volume,  $R$  is the distance of the detector from the diffracting specimen,  $\theta$  is the Bragg angle and  $m$  is the electron mass. Taking the ratio of the integrated intensity for the  $\text{CuK}_\alpha$  component to the integrated intensity of the  $\text{CuK}_\beta$  component, as in the case of the single crystal, one obtains after a slight rearrangement:

$$\frac{A_{\alpha P}}{A_{\beta P}} = \frac{I_{\alpha}}{I_{\beta}} \left( \frac{1 + \cos^2 2\theta_\alpha}{\sin^2 \theta_\alpha \cos \theta_\alpha} \right) \left( \frac{1 + \cos^2 2\theta_\beta}{\sin^2 \theta_\beta \cos \theta_\beta} \right)^{-1} \quad (11)$$

where  $A_{\alpha P}$  and  $A_{\beta P}$  are the measured areas under the peak intensity curves for diffraction of the  $\text{K}_\alpha$  and  $\text{K}_\beta$  wavelengths by the powder sample. The wavelengths and the absorption coefficients drop out because  $\lambda^2$  is proportional to  $\mu$ .

Using equation (11) and the measured areas  $A_{\alpha P}$ ,  $A_{\beta P}$  for the reflections from the  $(1\bar{1}00)$  and  $(1\bar{1}01)$  planes a mean value of  $I_{\alpha}/I_{\beta}$  was found to be 5.00. Knowing this ratio, and hence its reciprocal, the value of the parameter in equation (10) could be determined for each set of diffracting planes.

Using a range of values of  $\epsilon$  suggested by the theoretical calculations, for each set of planes, the quantities of  $Q_\alpha$  and  $Q_\beta$  were calculated as functions of  $\epsilon$ . The procedure is demonstrated below for the  $(3\bar{3}01)$  planes.

The linear absorption coefficients for quartz were found by calculation to be  $92.51 \text{ cm}^{-1}$  and  $68.03 \text{ cm}^{-1}$  for the  $\text{CuK}_\alpha$  and  $\text{CuK}_\beta$  radiations, respectively. Now,  $\frac{\lambda_\beta}{\lambda_\alpha} = 0.8154$  where  $\lambda_\alpha = 1.542 \text{ \AA}$ ,  $\lambda_\beta = 1.392 \text{ \AA}$ ,  $I_{\beta P}/I_{\alpha P} = 1/5.00$  and the mean thickness of the crystal is  $t_0 = 0.0686 \text{ cm}$ .

For the  $(3\bar{3}01)$  planes  $\sin 2\theta_\alpha / \sin 2\theta_\rho = 1.063$ ,  $\mu_{o\alpha} t_\alpha = 7.665$ ,  $\mu_{o\rho} t_\rho = 5.113$ ,  $\frac{\text{Exp}(-\mu_{o\alpha} t_\alpha)}{\text{Exp}(-\mu_{o\rho} t_\rho)} = 9.395$  where  $t_\alpha = t_o / \cos \theta_\alpha$ ,  $t_\rho = t_o / \cos \theta_\rho$ ; and  $A_\alpha / A_\rho = 2.771$ . Hence, from the definition of  $K$  it follows that  $K = 2.771 \times 1/5.00 \times 0.8154 \times 1.063 \times 9.395 = 4.518$ . Also,  $P_\alpha = \cos 2\theta_\alpha = 0.3697$ ,  $P_\rho = \cos 2\theta_\rho = 0.4853$ .

Table IV. The procedure for calculating  $Q_\alpha$  and  $Q_\beta$  using the  $(3\bar{3}01)$  planes for illustration.

$\varepsilon$	$K_\alpha$	$F_\alpha K_\alpha$	$I_0(K_\alpha)$	$I_0(F_\alpha K_\alpha)$	$F_\alpha I_0(F_\alpha K_\alpha)$	$Q_\alpha$
0.65	4.98	1.84	26.76	2.04	0.755	27.52
0.67	5.13	1.90	30.80	2.13	0.787	31.69
0.70	5.36	1.98	37.64	2.25	0.831	38.47
0.72	5.52	2.04	43.20	2.344	0.866	44.07
0.74	5.67	2.10	49.70	2.45	0.904	50.60
0.76	5.82	2.15	57.40	2.54	0.0938	58.34
0.78	5.97	2.21	65.40	2.65	0.779	66.38
0.80	6.13	2.27	75.60	2.77	1.023	76.62
0.82	6.28	2.32	86.90	2.87	1.061	87.96
0.84	6.44	2.38	100.69	3.00	1.109	101.80
$\varepsilon$	$K_\beta$	$F_\beta K_\beta$	$I_0(K_\beta)$	$I_0(F_\beta K_\beta)$	$F_\beta I_0(F_\beta K_\beta)$	$Q_\beta$
0.65	3.52	1.71	7.50	1.88	0.910	8.41
0.67	3.62	1.76	8.16	1.94	0.940	9.10
0.70	3.79	1.84	9.44	2.04	0.991	10.43
0.72	3.90	1.89	10.37	2.11	1.025	11.39
0.74	4.00	1.94	11.30	2.19	1.061	12.36
0.76	4.11	1.99	12.43	2.26	1.099	13.53
0.78	4.22	2.05	13.68	2.36	1.146	14.82
0.80	4.33	2.10	15.06	2.45	1.187	16.24
0.82	4.44	2.15	16.58	2.54	1.233	17.81
0.84	4.55	2.21	18.27	2.65	1.286	19.56



Table V. Summary of Quantities for the  $(3\bar{3}01)$  planes, to be plotted on a graph.

$\epsilon$	$Q_\alpha$	$KQ_\beta$
0.65	27.52	38.00
0.67	31.69	41.11
0.70	38.47	47.12
0.72	44.07	51.46
0.74	50.60	55.84
0.76	58.34	61.13
0.78	66.38	66.96
0.80	76.62	73.37
0.82	87.96	80.46
0.84	101.80	88.36

The plots of  $Q_\alpha$  and  $KQ_\beta$  as functions of  $\epsilon$  were made and the values of  $\epsilon$  which satisfy equation (10) were found, as indicated earlier, from the points of intersection. The graphs are displayed on the pages which follow. Figure (6) applies to the typical calculations for the  $(3\bar{3}01)$  reflection shown in Tables IV and V.

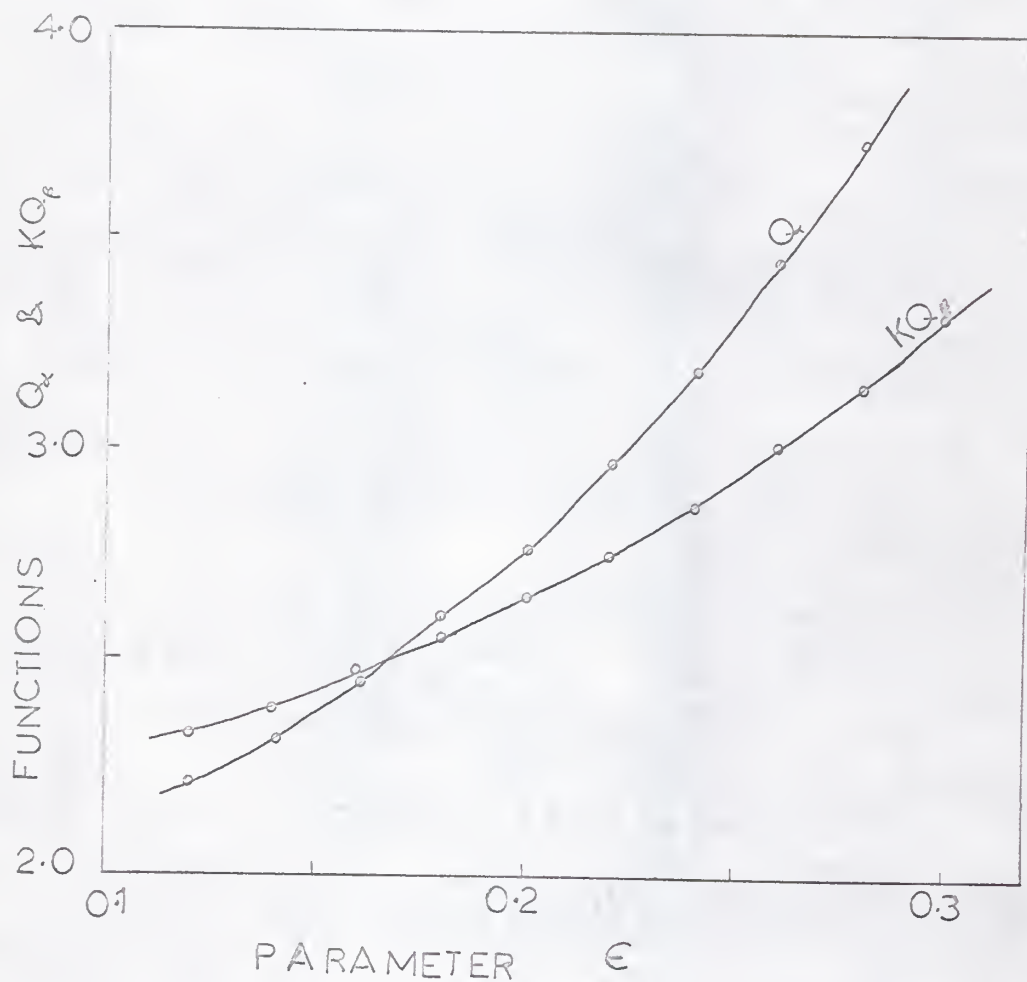


FIG. 2. Curves showing  $Q_\alpha$  and  $KQ_\beta$  as functions of  $\epsilon$  for the (1100) planes. The value of  $\epsilon$  which satisfies  $Q_\alpha = KQ_\beta$  is determined by the point of intersection.

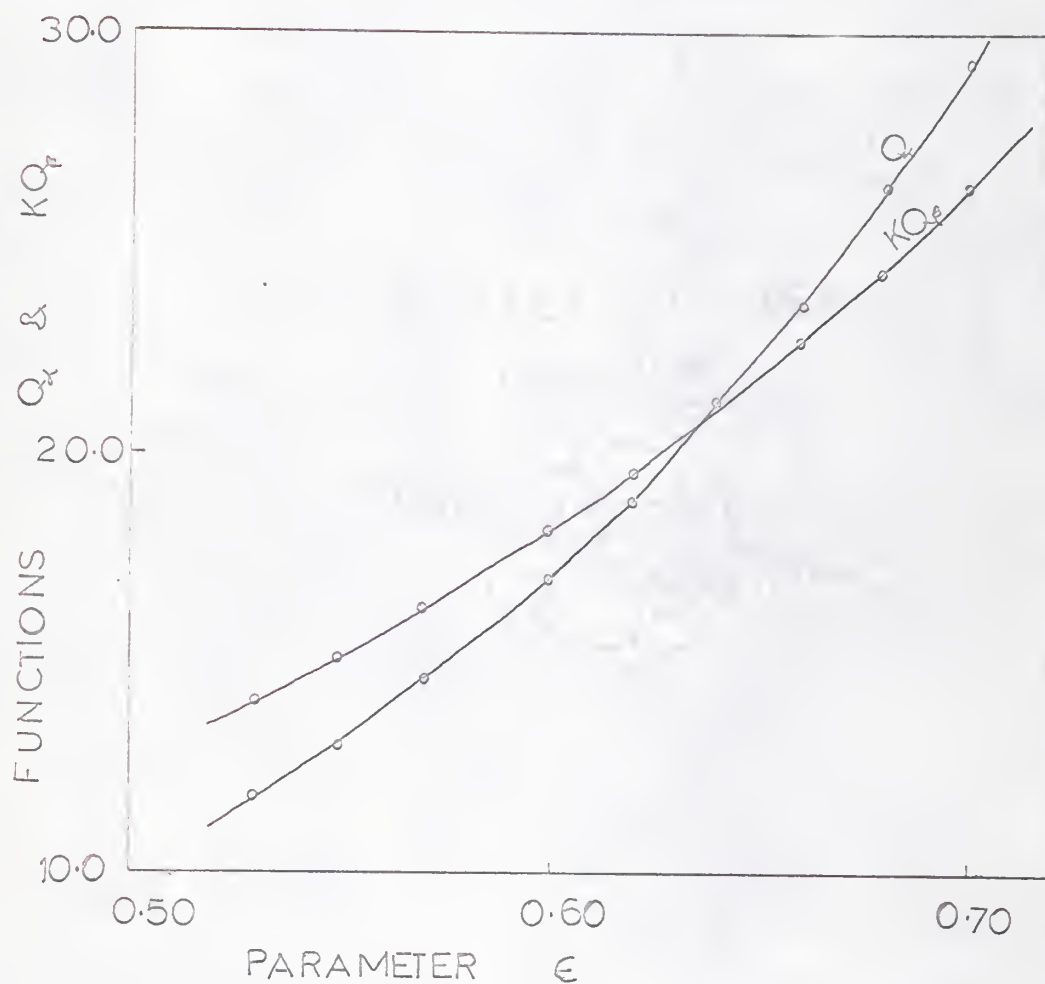


FIG. 3. Curves showing  $Q_\alpha$  and  $KQ_\beta$  as functions of  $\epsilon$  for the (1101) planes. The value of  $\epsilon$  which satisfies  $Q_\alpha = KQ_\beta$  is determined by the point of intersection.

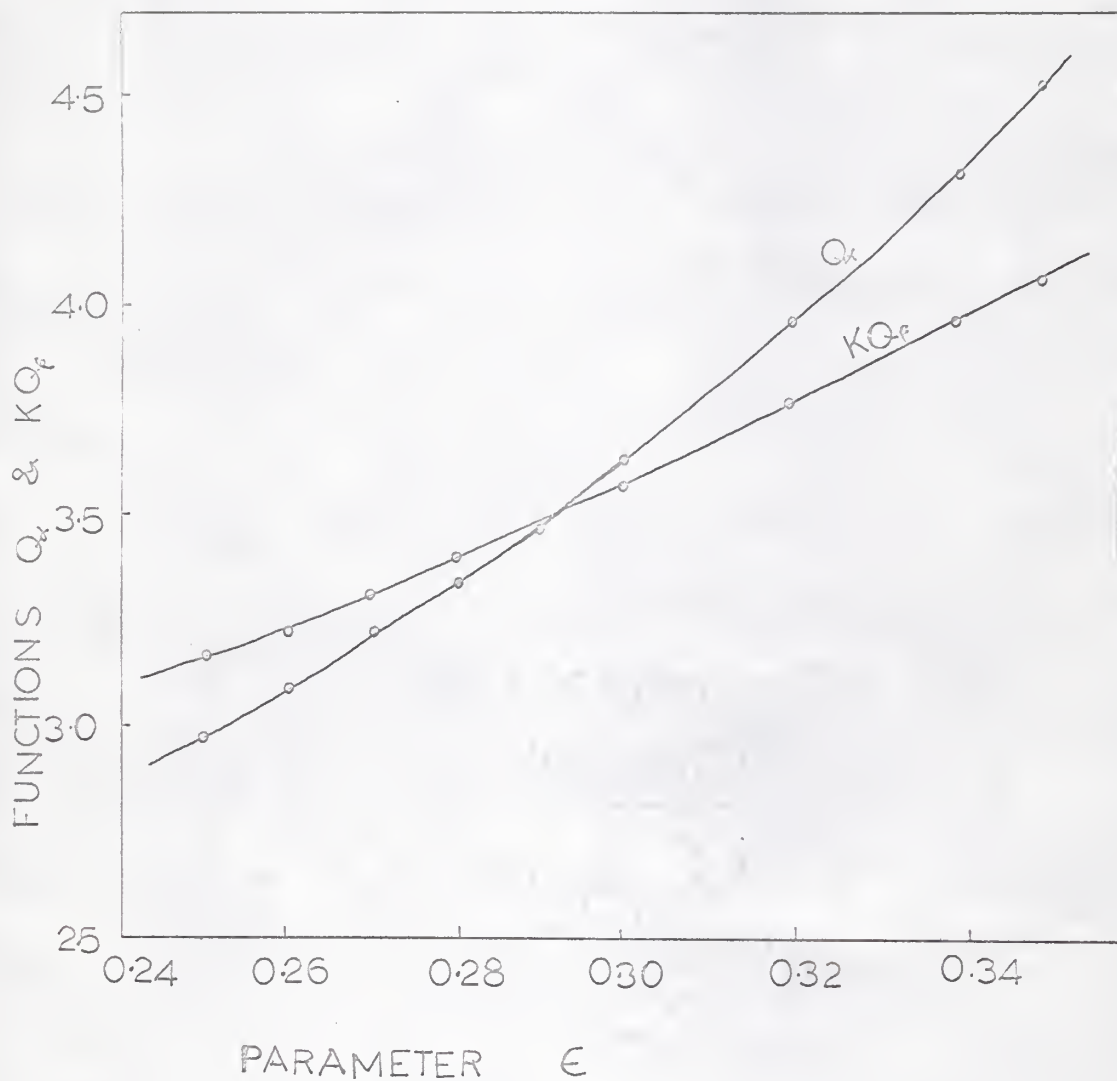


FIG. 4. Curves showing  $Q_\alpha$  and  $KQ_\beta$  as functions of  $\epsilon$  for the  $(1\bar{1}02)$  planes. The value of  $\epsilon$  which satisfies  $Q_\alpha = KQ_\beta$  is determined by the point of intersection.

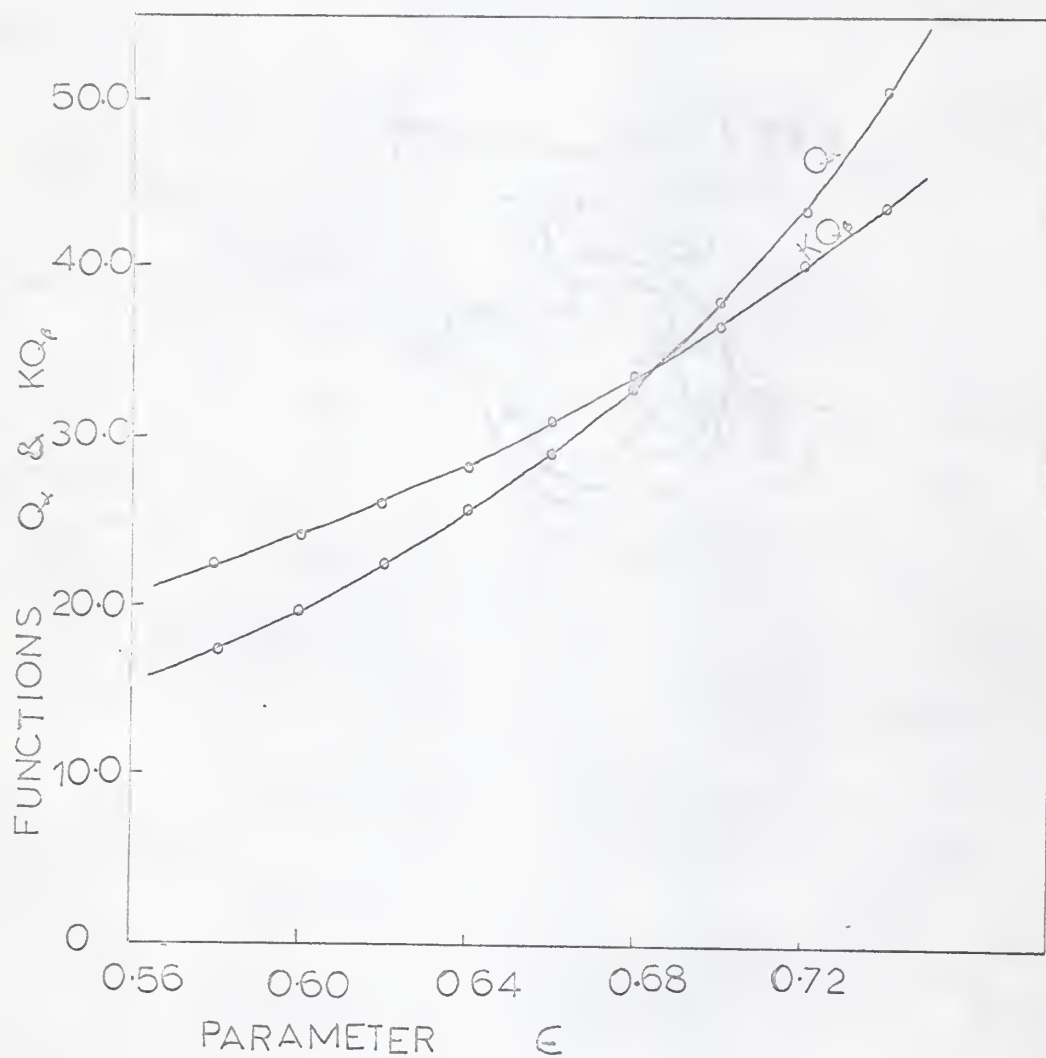


FIG. 5. Curves showing  $Q_\alpha$  and  $KQ_\beta$  as functions of  $\epsilon$  for the (2203) planes. The value of  $\epsilon$  which satisfies  $Q_\alpha = KQ_\beta$  is determined by the point of intersection.

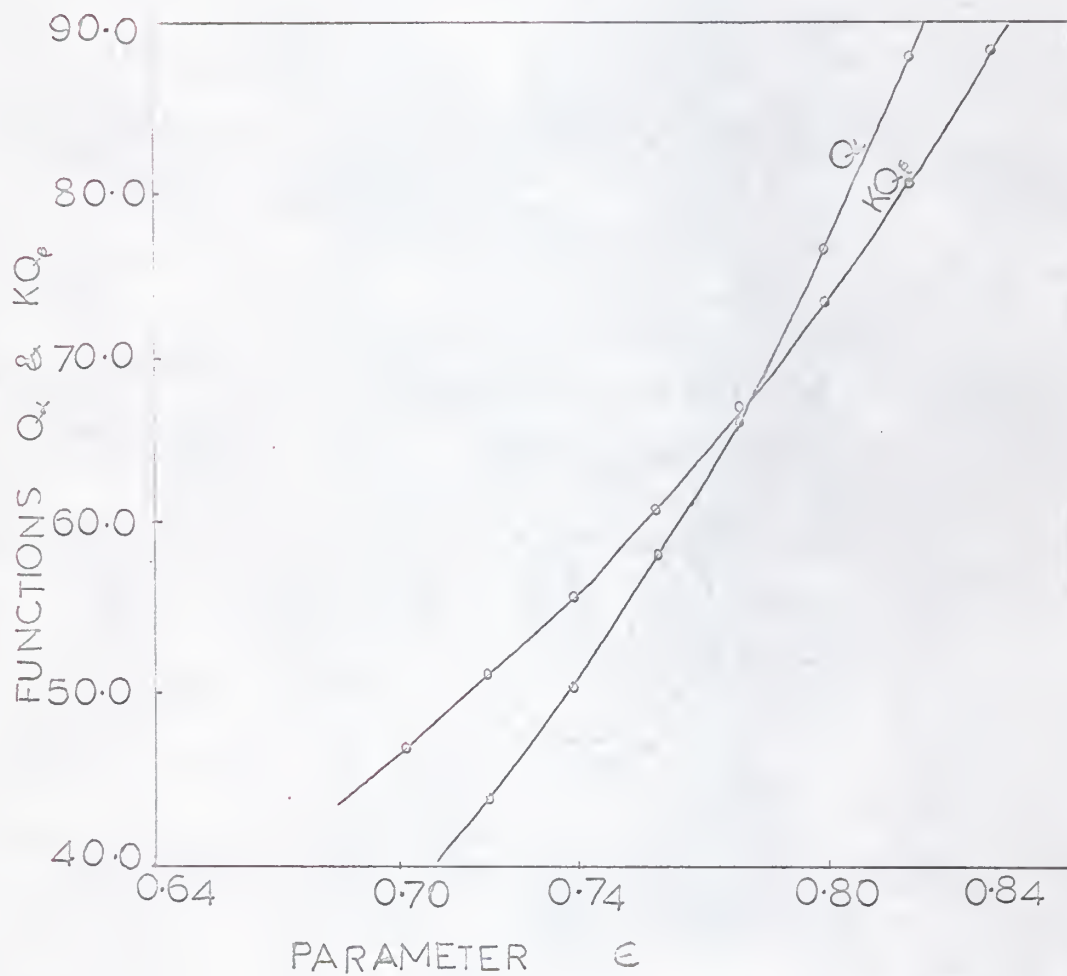


FIG. 6. Curves showing  $Q_\alpha$  and  $KQ_p$  as functions of  $\epsilon$  for the  $(\bar{3}\bar{3}01)$  planes. The value of  $\epsilon$  which satisfies  $Q_\alpha = KQ_p$  is determined by the point of intersection.



## DISCUSSION

The experimental and calculated values of  $\epsilon$  for each set of diffracting planes are given in Table VI below, together with the percentage difference of the experimental value from the calculated value. The Bragg angles  $\theta_x$ ,  $\theta_p$  are also given for each reflection.

Table VI. Summary of the experimental and theoretical values of epsilons for each reflection

Reflection	$\epsilon$ -experimental	$\epsilon$ -calculated	Difference %	$2\theta_x^\circ$	$2\theta_p^\circ$
1 $\bar{1}$ 00	0.168	0.276	39	20.83	18.81
1 $\bar{1}$ 01	0.638	0.686	7	26.64	24.02
1 $\bar{1}$ 02	0.293	0.287	2	39.45	35.52
2 $\bar{2}$ 03	0.684	0.655	4	68.13	60.83
3 $\bar{3}$ 01	0.782	0.774	1	68.30	60.97

Looking at this table, it is seen that the largest difference between the experimental and the calculated values of  $\epsilon$  occurs in the (1 $\bar{1}$ 00) reflection which has the smallest Bragg angle. The second largest departure is found in the (1 $\bar{1}$ 01) reflection which also has the second smallest Bragg angle. In addition, the experimental values of  $\epsilon$  for these two reflections are smaller than the calculated values, while for the high angle reflections (1 $\bar{1}$ 02), (2 $\bar{2}$ 03), (3 $\bar{3}$ 01) there is close agreement between the experimental and the calculated values: and the experimental values are slightly larger than the calculated values.

If the Kinematic Theory had been employed in the data analysis, the large

differences in the case of the small angle reflections could have been probably attributed to extinction; but in the dynamical theory used, extinction corrections are built in the theory. The  $(1\bar{1}01)$  happens to give the strongest diffracted intensity and although no analysis of experimental errors has been attempted here, on account of the rather involved method of extracting the values of  $\epsilon$  from the experimental data, it is unlikely that the difference between the two values of  $\epsilon$  for the  $(1\bar{1}00)$  reflection could be entirely due to experimental errors.

From all this, the question of temperature correction inevitably arises. The theoretical values of  $\epsilon$  were calculated on the assumption that the scattering atoms were stationary. The experimental investigations were carried out at room temperature when the atoms were vibrating about their mean positions of equilibrium. The effect of these vibrations is to reduce the observed intensities. For crystals with cubic symmetry and one-atom type, the correction factor, known as the Debye-Waller temperature factor, exists. However, for a hexagonal crystal like quartz with two atom types in the unit cell no exact correction factor has been worked out. The extent of the effect of atomic vibrations on the observed intensity depends on the nature of the atoms themselves and the relative positions these atoms occupy in the established radiation field. Now, in each of the five crystalline planes studied, the silicon and oxygen atoms occupy different relative positions in the wave field. It is tempting, therefore, to attribute the large difference between the theoretical and the experimental values of  $\epsilon$  to temperature effects.

The study of anomalous transmission, when fully developed, could lead to a variety of applications. For instance, the parameter  $\epsilon$  is related to the crystal structure factor by its very definition; and in the case of a centrosymmetric crystal  $\epsilon$  is proportional to the imaginary part of the structure

factor. Dreiling<sup>6</sup> shows how information on crystal structure factors could be inferred from the measurement of  $\epsilon$ .

Secondly, the anomalously transmitted intensities are greatly reduced by the presence of localized impurities or distortions in the crystal lattice. J. R. Patel and B. W. Batterman<sup>14</sup> show how this could be used as a sensitive tool for investigating small deviations that may occur in a nearly perfect crystal.

Thirdly, X-ray beams could be polarized by anomalous transmission technique. The radiation incident on a crystal slab has two components of polarization: the  $\sigma$ - and  $\pi$ -polarizations. The  $\sigma$ -polarization corresponds to the electric vector perpendicular to the plane of incidence, the  $\pi$ -polarization has the electric vector parallel to the plane of incidence. For a centrosymmetric crystal of sufficient thickness, the  $\pi$ -polarized component is attenuated in the crystal so much so that the transmitted radiation almost entirely consists of the  $\sigma$ -polarized component.

Indeed, when techniques for measuring the parameter  $\epsilon$  are perfected, agreement between the experimental and theoretical values of this parameter would give an experimental basis to the dynamical theory.

## SUMMARY

In this thesis those aspects of the dynamical theory of X-ray diffraction necessary for the calculation of the parameter  $\epsilon$  have been given. The parameter  $\epsilon$  has been seen to be the amount by which the coefficient of linear absorption is reduced. The values of  $\epsilon$  have been calculated for the atomic planes  $(1\bar{1}00)$ ,  $(1\bar{1}01)$ ,  $(1\bar{1}02)$ ,  $(2\bar{2}03)$ ,  $(3\bar{3}01)$  which happen to give the strongest diffracted intensities in  $\alpha$ -quartz. The experimental procedure which was followed to determine the values of  $\epsilon$  for the same atomic planes has been described. The integrated diffracted intensities when the crystal was set for Laue diffraction were measured for each of the five reflections. The ratio of the  $\text{CuK}_\alpha$  to the  $\text{CuK}_\beta$  components in the incident beam was determined from a separate experiment on powder quartz crystals. The results of the single crystal and the powder experiments were combined to determine the  $\epsilon$ 's for the five reflections in the manner described in the section on data analysis. The theoretical values and the experimentally determined values of  $\epsilon$  for each reflection are given in Table VI.

Good agreement between the experimental and the theoretical values of  $\epsilon$  for the reflections  $(1\bar{1}02)$ ,  $(2\bar{2}03)$  and  $(3\bar{3}01)$  exists. For the reflection  $(1\bar{1}01)$  the difference between the two values is rather large. The most serious disagreement is in the  $(1\bar{1}00)$  reflection. The disagreement between the theoretical and experimental values has been speculatively attributed to the lack of a procedure for obtaining the temperature correction factor for the hexagonal, polyatomic crystal like quartz. However, this does not rule out the inevitable experimental errors such as those involved in the measurement of the integrated intensities, where in some cases there was no clear demarcation for the contribution from the background radiation. Although the

peak intensities were sharp and appeared at the appropriate Bragg angles, indicating that the crystal was well aligned, this does not rule out completely those errors due to slight misalignment. Dreiling<sup>6</sup> shows that the values of  $\epsilon$  are not very sensitive to the existence of a wedge in the crystal slab.

The purpose of this thesis was to compare the predictions of the dynamical theory of X-ray diffraction about the values of  $\epsilon$  for the five reflections ( $1\bar{1}00$ ), ( $1\bar{1}01$ ), ( $1\bar{1}02$ ), ( $2\bar{2}03$ ) and ( $3\bar{3}01$ ) in  $\alpha$ -quartz with those experimentally determined. Quartz was chosen because it is a non-centrosymmetric, non-cubic, polyatomic crystal. All the published papers on the measurement of  $\epsilon$  have been about cubic, centrosymmetric, monoatomic crystals such as germanium, silicon, and copper. Good agreement has been obtained for the three high angle reflections, but serious disagreement has been observed for the small angle reflection ( $1\bar{1}00$ ). Since no formula for the temperature correction factor for a non-cubic, polyatomic crystal is known to the author, a further investigation is necessary to determine this factor experimentally by studying the variation of the diffracted intensities with temperature. The question of the positions of the silicon and oxygen atoms in the wave field, for each reflection, has not been examined: this needs to be investigated. When these aspects are studied, closer agreement between theory and experiment may be achieved.



## ACKNOWLEDGMENT

The author wishes to express his gratitude to Professor R. D. Dragsdorf who initiated the problem which has been the subject of this thesis, and for his guidance throughout the investigation. Gratitude is due also to Dr. Mark Dreiling who was very helpful to the author during the initial stages of the investigation. Like the author, Dr. Dreiling enjoyed the privilege of being a student of Professor Dragsdorf. The Bell Telephone Laboratories are acknowledged for kindly providing the quartz crystal.



## REFERENCES

1. Batterman, B. W. and Cole, H. Rev. Mod. Phys., 36, 681 (1964)
2. Batterman B. W., Phys. Rev., 129, 1416 (1962)
3. Borrmann, G. Z., Physik, 42, 157 (1941)
4. Cullity, B. D. Elements of X-Ray Diffraction  
Addison-Wesley Publishing Company, Inc.  
Reading, Massachusetts (1959)
5. Darwin, C. G. Phil. Mag., 27, 315 (1914)
6. Dreiling, M. J., Ph. D. Thesis (1967) Kansas State University
7. Ewald, P. P., Ann. Physik, 49, 1 (1916)
8. Freeman, A. J., Acta Cryst., 12, 933 (1959)
9. Hirsch, P. B., Acta Cryst., 5, 176, (1952)
10. Hunter, L. P., IBM Journal (April 1959)
11. James, R. W., The Optical Principles of the Diffraction of X-Rays  
A. Bell and Sons, London (1954)
12. Kato, N., J. Phys. Soc. of Japan, 10, 1 (1955)
13. Parratt, L. G. and Hempstead, C. F., Phys. Rev., 94, 1593 (1954)
14. Patel, J. R. and Batterman, B. W., J. App. Phys., 34, 2716 (1963)
15. Wyckoff, R. W. G., Crystal Structures  
Interscience Publishers, New York
16. Zachariasen, W. H., Theory of X-Ray Diffraction in Crystals  
John Wiley and Sons, New York (1945)

ANOMALOUS X-RAY TRANSMISSION BY A QUARTZ SINGLE CRYSTAL

by

JESUDAS MWANJE

B. Sc., University of East Africa, Makerere, 1966

---

AN ABSTRACT OF  
A MASTER'S THESIS

submitted in partial fulfillment of the  
requirements for the degree

MASTER OF SCIENCE

Department of Physics

KANSAS STATE UNIVERSITY  
Manhattan, Kansas

1968

Large, nearly perfect single crystals can, under suitable arrangement, transmit x-ray radiation with greatly reduced absorption. A parameter  $\epsilon$  (epsilon) which characterizes this reduction in absorption was calculated for the following diffracting atomic planes of the non-centrosymmetric, poly-atomic  $\alpha$ -quartz single crystal, using the Dynamical Theory of x-ray diffraction:  $(1\bar{1}00)$ ,  $(1\bar{1}01)$ ,  $(1\bar{1}02)$ ,  $(2\bar{2}03)$ ,  $(3\bar{3}01)$ . The same values were determined experimentally at room temperature in order to compare the theoretical predictions with experimental results. Good agreement between theoretical and experimental values of  $\epsilon$  was obtained for all the planes with the exception of the  $(1\bar{1}00)$  planes.